J|A|C|S
ARTICLES
Published on Web 12/02/2003

Polymorphic Forms of a Gold(I) Arylacetylide Complex with Contrasting Phosphorescent Characteristics

Wei Lu, Nianyong Zhu, and Chi-Ming Che*

Contribution from Department of Chemistry and HKU−CAS Joint Laboratory on New Materials, The University of Hong Kong, Pokfulam Road, Hong Kong SAR, China

Received August 31, 2003; E-mail: cmche@hku.hk

Abstract: The spectroscopic properties and crystal structures of the gold(I) arylacetylide complexes [(R_3P)-Au(C≡CAr)] (R = Cy, Ar = 4-nitrophenyl, **1**; 4-trifluoromethylphenyl, **2**; pentafluorophenyl, **3**; R = Ph, Ar = 4-nitrophenyl, **4**) have been examined. The dipole-allowed and -forbidden transitions of **1** (**4** in parentheses) at λ_{max} 340 (336) and ca. 485 (470) nm in CH_2Cl_2 solution at 298 K are assigned to the singlet and triplet intraligand charge transfer (ILCT) transitions of the 4-nitrophenylacetylide moiety, whereas **2** (**3** in parentheses**)** shows localized singlet and triplet acetylenic $\pi\pi^*$ transitions at λ_{max} 287 (276) and 426 nm, respectively. Two polymorphs of **1** with contrasting phosphorescent characteristics have been identified. At 298 K, the emissive form of **1**, as well as **2**−**4**, are highly phosphorescent with peak maximum at 504, 425, 521, and 495 nm, respectively; the other polymorph of **1** is nonemissive at 298 K but emission is detected at 77 K with peak maximum at 486 nm. Crystallographic studies reveal that the major differences between the emissive and nonemissive forms of **1** are the orientations of the molecular dipoles and the dihedral angles between neighboring 4-nitrophenyl moieties. Crystal **2** is isostructural to the nonemissive form of **1**, but does not display polymorphism. The molecular planes of two neighboring lumophores are coplanar in the emissive form of **1**, parallel in **4**, and nearly perpendicular (78.6°) to each other in the nonemissive form of **1**. Both the nature of the excited state and the dihedral angle between adjacent [Au-(C≡CAr)] moieties determine the phosphorescent properties of these molecular crystals.

Introduction

The spontaneous aggregation of two-coordinate gold(I) complexes in the solid state and in fluid and glassy solutions has generated considerable interest in recent years.[1] Numerous studies have revealed that aurophilic interactions, which are observed to be sensitive to the presence and nature of counterions and solvent molecules in the crystal lattice, play a key role in the structural and luminescent properties of gold(I) solids. There are several reports in the literature on the polymorphism (the occurrence of different crystalline forms with the same chemical components) of luminescent gold(I) complexes with or without close Au···Au contacts (shorter than 3.6 Å). For the two polymorphs of [$(CyNC)_2Au$]PF_6 (Cy = cyclohexyl) isolated by Balch and co-workers,[2] one is colorless and emits at λ_{max} 424 nm while the other is yellow and emits at λ_{max} 480 nm. The crystallographical findings revealed that the colorless form contains linear chains of Au···Au interactions (ca. 3.18 Å), whereas shorter Au···Au contacts (ca. 2.97 Å) are evident in the yellow form. The solid-state luminescent behavior of these polymorphs are reported to be dependent on the nature and configuration of the infinite gold(I) chains arising from attractive aurophilic interactions in the crystal lattices. Regarding the two colorless polymorphic forms of crystalline [(Ph_3As)AuCl],[3] which are needle- and prism-shaped, both emit with peak maxima at ca. 360 nm at ambient temperature, and a phenyl-localized $^3\pi\pi^*$ excited state has been assigned. Crystallographic studies on these two crystal forms showed that they exist in the same orthorhombic $P2_12_12_1$ space group but differ slightly in the intramolecular orientation of the phenyl groups and the intermolecular crystal packing. Interestingly, appreciable Au···Au interactions were absent from these two polymorphs.

Excitonic coupling[4] between nonconjugated organic chromophores is normally encountered in the condensed phase,[5] and is cited to account for aggregation-induced fluorescence enhancement in organic lumophores.[6] Such phenomenon, however, has not been reported for phosphorescent metal-organic compounds, which have been intensely studied as potential elec-

(1) (a) Schmidbaur, H., Ed.; *Gold: Progress in Chemistry, Biochemistry and Technology*; John Wiley & Sons: Chichester, 1999. Schmidbaur, H. *Chem. Soc. Rev.* **1995**, *24*, 391−400. (b) Pathaneni, S. S.; Desiraju, G. R. *J. Chem. Soc., Dalton Trans.* **1993**, 319−322. (c) Yam, V. W. W.; Li, C. K.; Chan, C. L. *Angew. Chem., Int. Ed.* **1998**, *37*, 2857−2859. (d) Fu, W. F.; Chan, K. C.; Miskowski, V. M.; Che, C. M. *Angew. Chem., Int. Ed.* **1999**, *38*, 2783−2785. (e) Vickery, J. C.; Olmstead, M. M.; Fung, E. Y.; Balch, A. L. *Angew. Chem., Int. Ed. Engl.* **1997**, *36*, 1179−1181. (f) Lee, Y.; McGarrah, J. E.; Lachicotte, R. J.; Eisenberg. R. *J. Am. Chem. Soc.* **2002**, *124*, 10 662−10 663.

(2) White-Morris, R. L.; Olmstead, M. M.; Balch, A. L. *J. Am. Chem. Soc.* **2003**, *125*, 1033−1040.

(3) (a) Weissbart, B.; Larson, L. J.; Olmstead, M. M.; Nash, C. P.; Tinti, D. S. *Inorg. Chem.* **1995**, *34*, 393−395. (b) Larson, L. J.; McClauley, E. M.; Weissbart, B.; Tinti, D. S. *J. Phys. Chem.* **1995**, *99*, 7218−7226.

(4) (a) McRae, E. G.; Kasha, M. *J. Chem. Phys.* **1958**, *28*, 721−722. (b) Kasha, M.; Rawls, H. R.; El-Bayoumi, M. A. *Pure Appl. Chem.* **1965**, *11*, 371−392.

(5) Recent examples: (a) Liang, K.; Farahat, M. S.; Perlstein, J.; Law, K. Y.; Whitten, D. G. *J. Am. Chem. Soc.* **1997**, *119*, 830−831. (b) Piet, J. J.; Taylor, P. N.; Anderson, H. L.; Osuka, A.; Warman, J. M. *J. Am. Chem. Soc.* **2000**, *122*, 1749−1757. (c) Würthner, F.; Yao, S. *Angew. Chem., Int. Ed.* **2000**, *39*, 1978−1980. (d) Zeena, S.; Thomas, K. G. *J. Am. Chem. Soc.* **2001**, *123*, 7859−7865. (e) Ajayaghosh, A.; Arunkumar, E.; Daub, J. *Angew. Chem., Int. Ed.* **2002**, *41*, 1766−1769 and references therein.

Chart 1

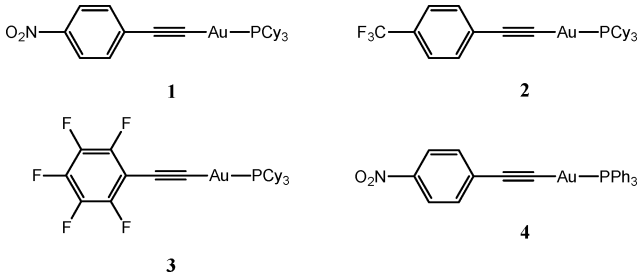

trophosphorescent dopants in high-performance organic light-emitting devices.[7] Excitonic coupling may provide a radiative pathway for interacting triplet emitters, thereby obviating the diminished efficiencies typically observed in devices with high emitter doping levels thought to arise from triplet−triplet annihilation.[7] Hence, the geometry and consequences of interactions between phosphorescent emitters in molecular crystals merit closer scrutiny, and the polymorphic forms of a metal-based lumophore with contrasting phosphorescent characteristics would be an ideal candidate for this purpose.

Gold(I) alkynyl compounds are of particular interest owing to their stability, ease of preparation, novel solid-state structures,[8] and interesting physical properties, such as nonlinear optical response,[9] liquid crystallinity,[10] and photoluminescence.[11,12] Very recently, several heterobimetallic complexes based on Au−C≡C ligation have been reported for application as potential optoelectronic materials.[13] Here, we report the intriguing solid-state emissive and structural properties of a phosphorescent polymorphic gold(I) complex, namely [(Cy_3P)-$AuC{\equiv}CC_6H_4$-4-NO_2] (Cy = cyclohexyl) (**1**) (Chart 1), where the heavy $[(Cy_3P)Au]^+$ moiety is employed to enhance spin−orbit coupling and the electron-withdrawing nitro group is introduced to increase the transition dipole moment of this lumophore. To the best of our knowledge, this is the first report of a polymorphic Au(I) complex without short Au···Au contacts in the crystal lattices that exhibits contrasting luminescent properties. Furthermore, the present study offers a rare opportunity to study excitonic coupling in a phosphorescent metal-organic compound. The derivatives **2**−**4** were studied for comparison and to probe the effects of the substituents on the arylacetylide and phosphine auxiliaries.

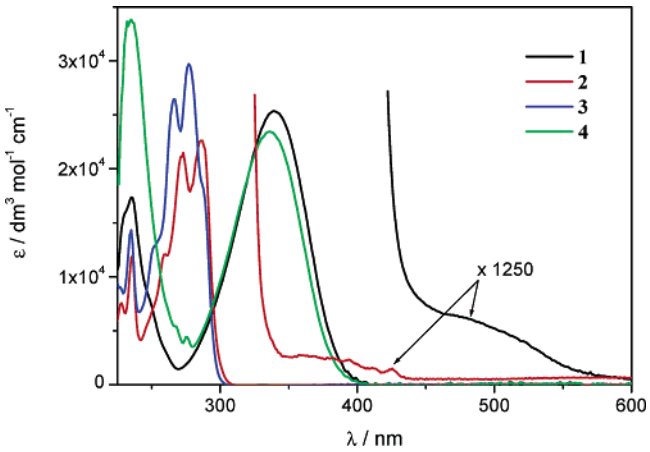

Figure 1. Absorption spectra of complexes **1**−**4** in CH_2Cl_2 at 298 K.

Results

Electronic Absorption Spectroscopy. The UV−vis absorption spectra of **1**−**4** in CH_2Cl_2 at 298 K are shown in Figure 1. There is an intense, structureless absorption band at λ_{max} 340 and 336 nm for **1** and **4**, respectively, with ϵ of ca. 2.5×10^4 $dm^3\ mol^{-1}\ cm^{-1}$. This band shows positive solvatochromism, thus the absorption maximum of **1** shifts from 336 to 340 nm when the solvent changes from toluene to CH_2Cl_2. In addition to this high-energy band, there is a weak absorption shoulder at around 485 nm ($\epsilon \approx 5$ $dm^3\ mol^{-1}\ cm^{-1}$) for **1** and 470 nm ($\epsilon \approx 3$ $dm^3\ mol^{-1}\ cm^{-1}$) for **4**. We tentatively assign the 340 and 485 nm bands of **1** to the singlet and triplet intraligand charge transfer (ILCT) transition, respectively. On the basis of the absorption spectrum of **1**, the transition dipole moment of the lowest singlet excited state ($\mathbf{P}_{01}$) in CH_2Cl_2 solution at 298 K was calculated to be ca. 6.6 D according to eq 1[14]

$$\mathbf{P}_{01}{}^2 = (9.166 \times 10^{-3}) \int \epsilon(\nu) \mathrm{d}\nu/\nu_m \qquad (1)$$

where $\epsilon(\nu)$ is the molar extinction coefficient at wavenumber ν, and ν_m is the position of absorption maximum. For **2** and **3**, there is a structured absorption band with λ_{0-0} at 287 and 276 (with 285 nm shoulder) nm, and ϵ of ca. 2.3×10^4 and 3.0×10^4 $dm^3\ mol^{-1}\ cm^{-1}$, respectively. This band shows negative solvatochromism; thus the absorption maximum shifts from 289 to 287 and 283 nm for **2** and from 277 to 276 and 289 nm for **3**, when the solvent changes from toluene to CH_2Cl_2 and EtOH. The salient vibrational spacings of these bands are 1830 (for **2**) and 1930 (for **3**) cm^{-1}, which fall in the range expected for C≡C stretching in the excited state, and hence these bands are

(6) (a) Zahn, S.; Swager, T. M. *Angew. Chem., Int. Ed.* **2002**, *41*, 4225−4230. (b) An, B. K.; Kwon, S. K.; Jung, S. D.; Park, S. Y. *J. Am. Chem. Soc.* **2002**, *124*, 14 410−14 415.
(7) Baldo, M. A.; O'Brien, D. F.; You, Y.; Shoustikov, A.; Sibley, S.; Thompson, M. E.; Forrest, S. R. *Nature* **1998**, *395*, 151−154.
(8) (a) Müller, T. E.; Mingos, D. M. P.; Williams, D. J. *J. Chem. Soc., Chem. Commun.* **1994**, 1787−1788. (b) Mingos, D. M. P.; Yau, J.; Menzer, S.; Williams, D. J. *Angew. Chem., Int. Ed. Engl.* **1995**, *34*, 1894−1895. (c) Vicente, J.; Chicote, M.-T.; Abrisqueta, M.-D.; Guerrero, R.; Jones, P. G. *Angew. Chem., Int. Ed. Engl.* **1997**, *36*, 1203−1204. (d) McArdle, C. P.; Irwin, M. J.; Jennings, M. C.; Puddephatt, R. J. *Angew. Chem., Int. Ed.* **1999**, *38*, 3376−3378. (e) McArdle, C. P.; Vittal, J. J.; Puddephatt, R. J. *Angew. Chem., Int. Ed.* **2000**, *39*, 3819−3822.
(9) Donor−acceptor Au(I) acetylides have been intensely studied by Humphrey and co-workers as NLO materials, for example: (a) Whittall, I. R.; Humphrey, M. G.; Samoc, M.; Luther-Davies, B. *Angew. Chem., Int. Ed. Engl.* **1997**, *36*, 370−372. (b) Whittall, I. R.; Humphrey, M. G.; Samoc, M.; Luther-Davies, B.; Hockless, D. C. R. *J. Organomet. Chem.* **1997**, *544*, 189−196.
(10) Kaharu, T.; Ishii, R.; Adachi, T.; Yoshida, T.; Takahashi, S. *J. Mater. Chem.* **1995**, *5*, 687−692.
(11) (a) Jia, G.; Puddephatt, R. J.; Scott, J. D.; Vittal, J. J. *Organometallics* **1993**, *12*, 3565−3574. (b) Yam, V. W. W.; Choi, S. W. K. *J. Chem. Soc., Dalton Trans.* **1996**, 4227−4232. Irwin, M. J.; Vittal, J. J.; Puddephatt, R. J. *Organometallics* **1997**, *16*, 3541−3547. (c) Vicente, J.; Chicote, M. T.; Abrisqueta, M. D.; Jones, P. G. *Organometallics* **1997**, *16*, 5628−5636. (d) Wang, H. M. J.; Chen, C. Y. L.; Lin, I. J. B. *Organometallics* **1999**, *18*, 1216−1223.
(12) (a) Li, D.; Che, C. M.; Lo, W. C.; Peng, S. M. *J. Chem. Soc., Dalton Trans.* **1993**, 2929−2932. (b) Xiao, H.; Cheung, K. K.; Guo, C. X.; Che, C. M. *J. Chem. Soc., Dalton Trans.* **1994**, 1867−1871. (c) Xiao, H.; Weng, Y. X.; Peng, S. M.; Che, C. M. *J. Chem. Soc., Dalton Trans.* **1996**, 3155−3157. (d) Che, C. M.; Chao, H. Y.; Miskowski, V. M.; Li, Y.; Cheung, K. K. *J. Am. Chem. Soc.* **2001**, *123*, 4985−4991. (e) Lu, W.; Xiang, H. F.; Zhu, N.; Che, C. M. *Organometallics* **2002**, *21*, 2343−2346. (f) Chao, H. Y.; Lu, W.; Li, Y.; Chan, M. C. W.; Che, C. M.; Cheung, K. K.; Zhu, N. *J. Am. Chem. Soc.* **2002**, *124*, 14 696−14 706. (g) Lu, W.; Zhu, N.; Che, C. M. *J. Organomet. Chem.* **2003**, *670*, 11−16.
(13) (a) Back, S.; Gossage, R. A.; Lang, H.; van Koten, G. *Eur. J. Inorg. Chem.* **2000**, 1457−1464. (b) Shiotsuka, M.; Yamamoto, Y.; Okuno, S.; Kitou, M.; Nozaki, K.; Onaka, S. *Chem. Commun.* **2002**, 590−591.
(14) (a) Turro, N. J. *Modern Molecular Photochemistry*; The Benjamin/Cummings Publishing Co., Inc.: Menlo Park, CA, 1978; Chapter 5. (b) Levitsky, I. A.; Kishikawa, K.; Eichhorn, S. H.; Swager, T. M. *J. Am. Chem. Soc.* **2000**, *122*, 2474−2479.

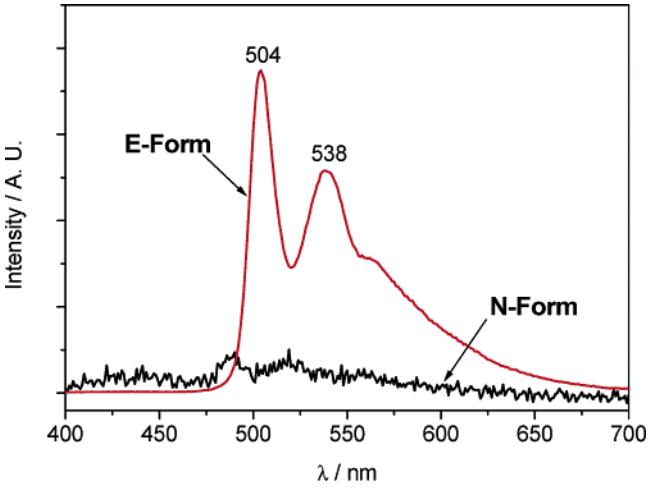

Figure 2. Solid-state emission spectra (λ_{ex} = 330 nm) of the E- and N-forms of **1** at 298 K.

assigned as predominantly $^1(\pi\pi^*)$ acetylenic transitions. In addition to this high-energy absorption band, **2** exhibits a weak absorption beyond 350 nm with λ_{0-0} at 426 nm ($\epsilon \approx 2$ dm^3 mol^{-1} cm^{-1}), which is assigned to the localized $^3(\pi\pi^*)$ acetylenic transition.

Emission and Excitation Spectroscopy. Complex **1** is weakly emissive in fluid solutions at 298 K and the emission energy is dependent upon the solvent polarity; the emission maximum shifts from 492 to 524 and 545 nm from toluene to CH_2Cl_2 and EtOH, respectively. The positive solvatochromism (i.e., transition energy decreases with greater solvent polarity) indicates that the ground state is less polar than the excited state. This complex is strongly emissive in 77 K glassy toluene solution with λ_{0-0} at 491 nm. Two crystal forms of **1** were obtained upon slow diffusion of Et_2O into a CH_2Cl_2 solution. Both are yellow in color but one is rodlike and the other is platelike in shape. Under UV light illumination, the rodlike crystals (denoted as E-form) are strongly luminescent but the platelike ones (denoted as N-form) are virtually nonemissive. The E/N-form weight ratio after recrystallization is estimated to be 1/9. The contrasting emission properties between these two crystalline forms facilitated their separation by hand under UV illumination. The solid-state emission spectra of the E- and N-forms of **1** at 298 K are shown in Figure 2. The E-form emits intense greenish light with peak maxima at 504 and 538 nm (shoulder at ~560 nm); a vibronic progression of 1250 cm^{-1} is apparent, while the long lifetime (23 μs) suggests phosphorescence. We suggest that the emission originates from the triplet intraligand excited state (the absorption maximum of which occurs at around 485 nm in CH_2Cl_2 at 298 K). In contrast, the emission from N-form is exceedingly weak, with peak maxima at ca. 480 and 520 nm.

At 77 K, the E-form exhibits long-lived (335 μs) and highly structured emission, and two vibronic progressions, namely 1250 (major) and 2110 cm^{-1}, are apparent (Figure 3, top). Although the peak maximum appears at 512 nm, a distinct shoulder at 504 nm is observed, which matches the emission maximum found at 298 K (Figure 2). The excitation spectrum of the E-form gives a well-defined λ_{0-0} line at 499 nm together with vibronically structured bands in the 453−489 nm range. The N-form emits intensely at 77 K and shows a less-resolved emission spectrum with the λ_{0-0} line appearing at 486 nm

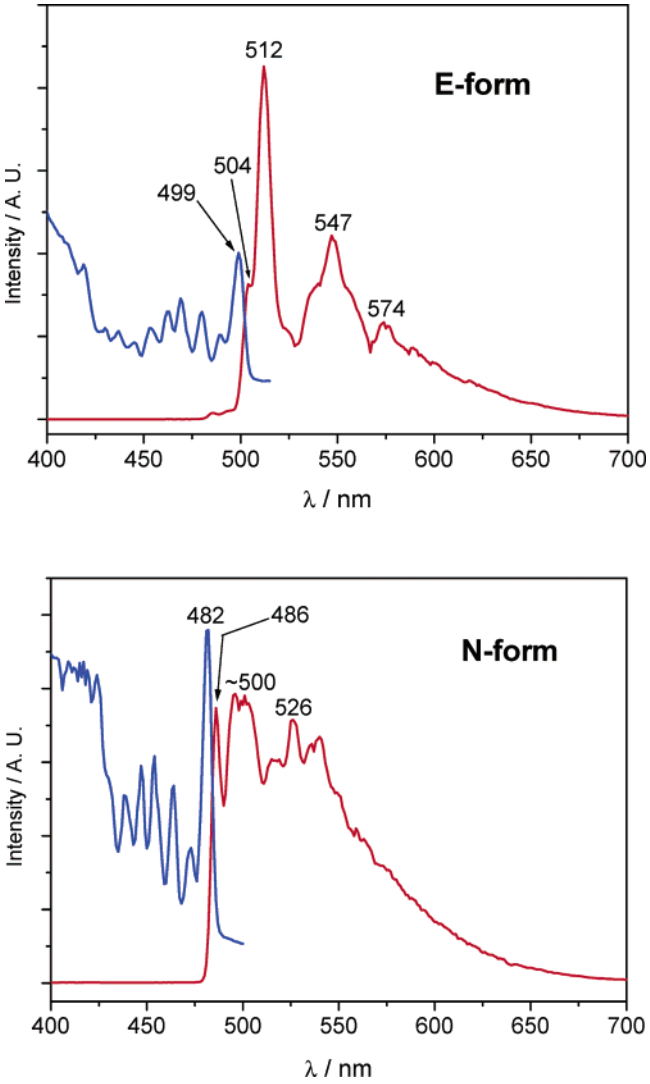

Figure 3. Solid-state emission and excitation spectra of the E- (top, λ_{ex} = 330 nm, λ_{em} = 547 nm) and N- (bottom, λ_{ex} = 350 nm, λ_{em} = 526 nm) forms of **1** at 77 K.

(Figure 3, bottom). This emission is also long-lived (193 μs) and can be similarly assigned to a triplet intraligand excited state like for the E-form. Furthermore, the excitation spectrum of the N-form exhibits a λ_{0-0} line at 482 nm, plus fine structures in the 438−473 nm range that are comparable in pattern to the excitation spectrum of the E-form. The blue-shifts (ca. 730 cm^{-1}) of peak maxima from the E- to the N-form, both for the emission and excitation spectra, together with the stark contrast between the luminescent properties of these two crystalline forms of **1** at 298 K, are unusual.

The emission and excitation spectra of complexes **2**−**4** are given in the Supporting Information. Complex **2** is highly emissive in fluid and alcoholic (methanol/ethanol = 1/4, v/v) glassy solutions (λ_{0-0} 426 nm) and in the solid state (λ_{0-0} 425 nm at 298 K). The emission maximum of **2** in toluene, CH_2Cl_2 and EtOH are virtually identical with λ_{max} at 426 nm, and a localized $^3\pi\pi$ excited state is assigned. Complex **3** is nonemissive in fluid solutions but a crystalline sample emits at λ_{max} 521 nm at 298 K and 490 nm at 77 K. In 77 K alcoholic glassy solution, **3** emits at λ_{0-0} 485 nm. The solvent-dependent emissive behavior of **4** in fluid solutions is similar to that of **1**; the emission maximum shifts from 486 to 514 and 534 nm from

Table 1. Crystal Data

	1 (E-form)	1 (N-form)	2	3	4
formula	$C_{26}H_{37}AuNO_2P$	$C_{26}H_{37}AuNO_2P$	$C_{27}H_{37}AuF_3P$	$C_{26}H_{33}AuF_5P$	$C_{26}H_{19}AuNO_2P$
fw	623.50	623.50	646.50	668.46	605.36
T, K	301(2)	301(2)	253(2)	253(2)	253(2)
color	yellow	yellow	colorless	colorless	yellow
crystal size	0.5 × 0.3 × 0.2	0.3 × 0.2 × 0.1	0.4 × 0.3 × 0.2	0.2 × 0.2 × 0.1	0.3 × 0.15 × 0.07
crystal system	triclinic	monoclinic	monoclinic	monoclinic	monoclinic
space group	P-1	$P2_1/c$	$P2_1/c$	$P2_1$	$P2_1/c$
a, Å	9.381(2)	12.258(3)	12.316(3)	11.573(2)	8.611(2)
b, Å	10.029(2)	16.590(3)	16.415(3)	8.533(2)	18.466(4)
c, Å	14.374(3)	12.550(3)	12.889(3)	14.077(3)	14.184(3)
α, deg	108.53(3)				
β, deg	93.02(3)	96.68(3)	98.54(3)	106.87(3)	91.28(3)
γ, deg	98.31(3)				
V, Å^3	1261.7(4)	2534.8(10)	2576.8(10)	1330.3(5)	2254.8(9)
Z	2	4	4	2	4
D_c, g cm^{-3}	1.641	1.634	1.666	1.669	1.783
μ, mm^{-1}	5.915	5.889	5.805	5.636	6.618
F(000)	620	1240	1280	656	1168
$2\theta_{max}$, deg	51.3	51.3	51.2	50.7	51.2
no. reflections	5915	15265	14096	8566	10341
no. independent reflections	3724 [*R*(int) = 0.030]	4479 [*R*(int) = 0.043]	4800 [*R*(int) = 0.048]	4561 [*R*(int) = 0.045]	3980 [*R*(int) = 0.044]
no. variables	280	280	289	298	280
GOF on F^2	0.93	1.09	1.11	1.03	0.99
R_1[a]	0.029	0.027	0.031	0.038	0.028
wR_2[b]	0.066	0.079	0.093	0.102	0.077
residual *ρ*, e Å^{-3}	+0.488, −1.161	+0.548, −1.540	+0.659, −1.687	+1.555, −1.776	+0.626, −1.058

[a] $R = \sum||F_o| - |F_c||/\sum|F_o|$. [b] $Rw = \{\sum[w(F_o^2 - F_c^2)^2]/\sum[w(F_o^2)^2]\}^{1/2}$.

toluene to CH_2Cl_2 and EtOH, respectively. A crystalline sample of **4** emits with λ_{0-0} at 495 nm at 298 K and 493 nm at 77 K. The excitation spectrum of this sample exhibits a λ_{0-0} line at 489 nm plus fine structures in the 437−480 nm range, and is similar in pattern to the excitation spectra of the E- and N-forms of **1**. Hence, polymorphism and opposing solid-state emissions such as that observed for **1** were not evident for complexes **2**−**4**.

Crystal Structures and Intermolecular Contacts. All crystals were obtained from CH_2Cl_2/Et_2O solutions. The crystal data are shown in Table 1. The bond distances and angles for these crystal structures are normal for gold(I) acetylide complexes,[15] which have been extensively documented in the literature, so we focus here on their crystal packing arrangements and short intermolecular contacts. The sum of van der Waals radii taken from Bondi's data[16] is 2.90 Å for H···C and 2.67 Å for H···F, hence intermolecular distances that are shorter than these values may be considered as weak interactions.

The crystal structures of the E- and N-forms of **1** are shown in Figures 4 and 5, respectively. No solvent molecules are present in their crystal lattices, hence the E- and N-forms of **1** are exact polymorphs. The E-form crystallizes in the triclinic *P*-1 space group. The nitro group is coplanar with the phenylacetylide moiety. Neighboring molecules are arranged in pairs with molecular dipoles in opposite directions. There are weak C−H···π(C≡C) contacts between H8 of the phenyl ring and C1 of the acetylide moiety (H···C(C≡C) 2.791 Å; C−H···C(C≡C) 158°). The two phenyl rings are coplanar and these discrete dimers are packed into parallel sheets in the crystal lattice (Figure 4, bottom). In contrast, the N-form crystallizes in the monoclinic $P2_1/c$ space group and shows an infinite slanted chainlike structure along the *c*-axis. Adjacent molecules

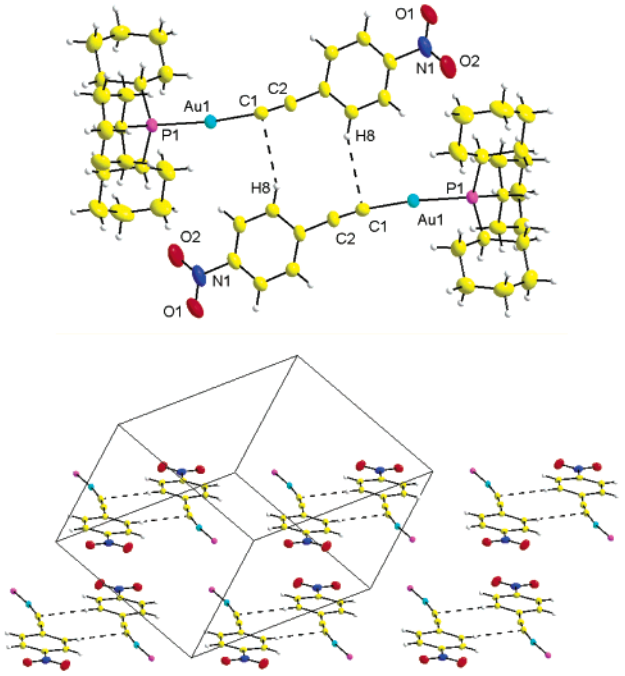

Figure 4. Crystal structure and packing diagram of the E-form of **1** with dashed lines indicating intermolecular contacts that are shorter than the sum of van der Waals radii.

are joined by C−H···π(C≡C) contacts between H7 of the phenyl ring and C1 of the acetylide group (H···C(C≡C) 2.810 Å; C−H···C(C≡C) 143°). The dihedral angle between adjacent phenyl rings is 79°, and the molecular dipoles are oriented in the same direction. Thus, *the major structural differences between the E- and N-form are the orientations of the molecular dipoles and the dihedral angles between neighboring 4-nitrophenyl moieties.*

(15) Transition metal acetylides: Manna, J.; John, K. D.; Hopkins, M. D. *Adv. Organomet. Chem.* **1995**, *38*, 79−154, and references therein.
(16) Bondi, A. *J. Phys. Chem.* **1964**, *68*, 441−451.

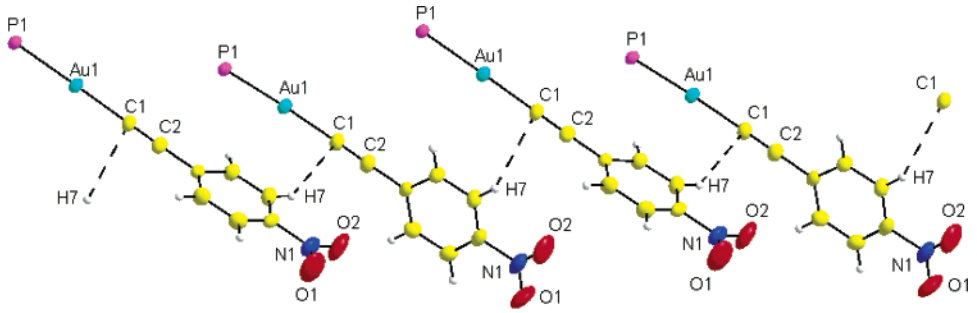

Figure 5. Crystal structures of the N-form of **1** (Cy groups are omitted for clarity) with dashed lines indicating intermolecular contacts that are shorter than the sum of van der Waals radii.

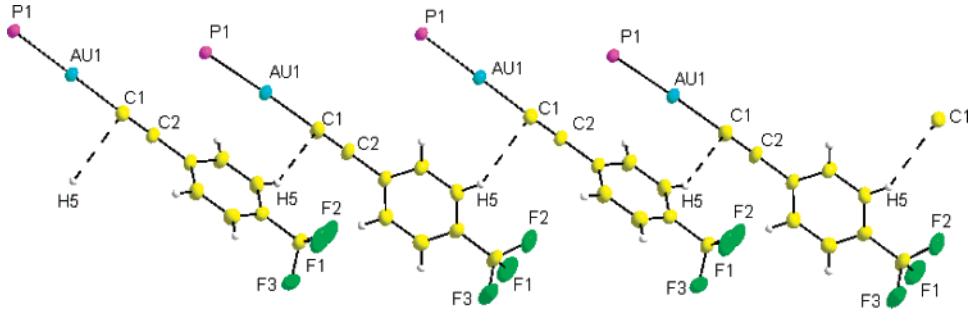

Figure 6. Crystal structures of **2** (Cy groups are omitted for clarity) with dashed lines indicating intermolecular contacts that are shorter than the sum of van der Waals radii.

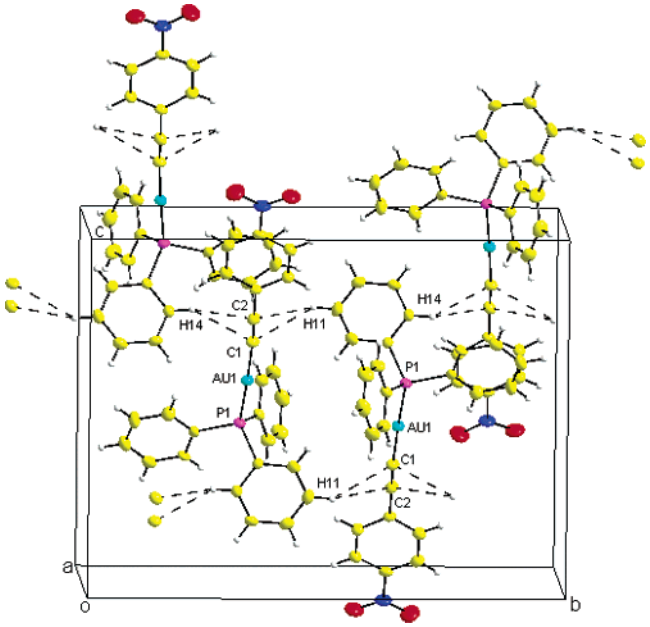

Figure 7. Unit cell of crystal **4** with dashed lines indicating the distances shorter than the sum of van der Waals radii.

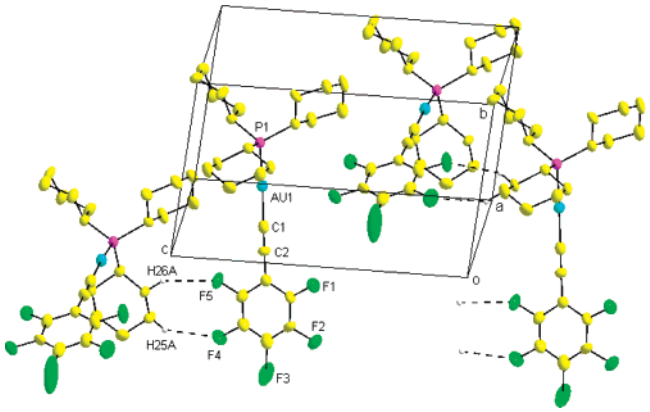

Figure 8. Unit cell of crystal **3** (only selected C−H···F−C contacts are shown for clarity).

Crystal **2** (Figure 6) exists in the monoclinic $P2_1/c$ space group and is isostructural to the N-form of **1**. The extent of isostructurality for these two crystals was calculated by the unit cell similarity index,[17] $\Pi = |1 - (a + b + c)/(a' + b' + c')|$ [where a, b, c, a', b' and c' are the orthogonalized lattice parameters of crystals **2** and **1** (N-form)], and the isostructurality index,[17] $I_i(n) = |1 - [\Sigma(\Delta R_i)^2/n]^{1/2}| \times 100$ [where n is the number of distance differences (ΔR_i) between the crystal coordinates of identical non-H atoms within the same section of the asymmetric units of crystals **2** and **1** (N-form)]. Values of Π close to zero and $I_i(n)$ approaching 100 implies isostructurality. The calculated value of Π and $I_i(21)$, for crystals **2** and **1** (N-form) is 0.004 and 97, respectively, suggesting excellent isostructurality. Furthermore, the molecular arrangement in the crystal lattice of **2** are identical to that of **1** (N-form). Thus neighboring molecules are joined by C−H···π(C≡C) contacts between H5 of the phenyl ring and C1 of the acetylide group (H···C(C≡C) 2.801 Å; C−H···C(C≡C) 147°), and the dihedral angle between adjacent phenyl rings is 89°.

The crystal structure of complex **4** was previously reported by Humphrey and co-workers[18] but the crystal packing was not mentioned, so in this work, this structure was re-determined. Crystal **4** (Figure 7) exists in the monoclinic $P2_1/c$ space group but the packing is different from those of **1** (N-form) and **2**. In

(17) Kálmán, A.; Párkányi, L.; Argay; G. *Acta Cryst.* **1993**, *B49*, 1039−1049.

(18) Whittall, I. R.; Humphrey, M. G.; Houbrechts, S.; Persoons, A.; Hockless, D. C. R. *Organometallics* **1996**, *15*, 5738−5745.

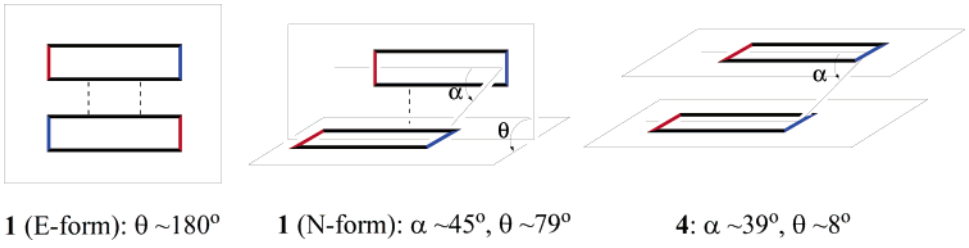

Figure 9. Schematic representations of geometry of adjacent lumophores in crystals **1** (E- and N-forms) and **4**. Bold squares represent the P−Au−C≡CC_6H_4-4-R (R = NO_2 or CF_3) moieties with the blue side indicating phosphine and the red side indicating R; plain squares represent the molecular planes of the arylacetylide ligands and dashed lines indicate C−H···π(C≡C) contacts.

the crystal lattice of **4**, one molecule is connected to two neighboring molecules by C−H···π(C≡C) contacts between H11 and H14 of the Ph_3P phenyl rings and C1 and C2 of the acetylide group (H···C(C≡C) 2.74−2.82 Å; C−H···C(C≡C) 139−140°). Adjacent 4-nitrophenyl moieties are nearly parallel, as indicated by the dihedral angle of 8°.

Intermolecular C−H···π(C≡C) contacts are not observed in the crystal lattice of **3** (Figure 8), which contains no protons on the perfluorinated phenylacetylide ligand for interaction with the C≡C moiety. Instead, there are extensive C−H···F−C contacts[19] between protons of the Cy_3P cyclohexyl groups and F atoms of the C_6H_5 moiety (H···F 2.56−2.62 Å; C−H···F 135−147°). The dihedral angle between neighboring pentafluorophenyl planes is 53°.

Discussion

Intrinsic Electronic Effects. $[(Cy_3P)Au]^+$ is isolobal to H^+,[1a,12d] and the former has recently been shown to induce phosphorescence in π-conjugated carbon-rich compounds through Au−C≡C ligation.[12d−g] In the discrete monomeric state of **1**, the excited 4-nitrophenylacetylide chromophore is expected to cross from the singlet to triplet state through efficient spin−orbit coupling that is enhanced by the $[(Cy_3P)Au]^+$ moiety. Indeed, the lowest $S_0 \rightarrow T_1$ transition of **1** has been observed at ca. 485 nm with an ϵ value of ca. 5 dm^{-3} mol^{-1} cm^{-1} in CH_2Cl_2 solution; this is substantially larger than those reported for spin-forbidden triplet absorptions of pure organic chromophores. Long-lived phosphorescence has been observed from this excited state. We adopt the λ_{0-0} of 491 nm recorded in toluene glass at 77 K as the S_0-T_1 energy gap for monomeric **1**.

Comparison of the emission properties between **1** and **2**, both of which contain an electron-withdrawing group at the 4-position of the phenylacetylide ligand, provide information regarding the effect of electronic factors upon the contrasting solid-state emissions exhibited by the polymorphs of **1**. The crystal packing and intermolecular interactions of the N-form of **1** are identical to those in crystal **2**, but their solid-state luminescent properties are distinctly different. The likelihood that lowest excited states in **1** (ILCT) and **2** (acetylenic $\pi\pi^*$) are different is indicated by the following: (1) the low-energy dipole-allowed transition band in the absorption spectrum is structureless for **1** but highly structured with acetylenic vibronic progression for **2**; and (2) the emission energy for **1** in fluid solution is solvent-sensitive but this is not the case for **2**. The extension of π-conjugation from the phenylacetylide moiety to the NO_2 unit in **1** but not the CF_3 group in **2** may account for this disparity. This conjugation is also signified by the crystal structures of both the E- and N-forms of **1**, where the nitro group is exactly coplanar with the phenylacetylide moiety. On the basis of this evidence, the magnitude of the transition dipole moment in **1** should be significantly larger than that in **2**.

Extrinsic Crystal-Packing Effects. The relationships between two neighboring molecules in crystals **1** (E- and N-forms) and **4** are schematically depicted in Figure 9. The [(Cy_3P)AuC≡CAr] molecules adopt a linear configuration and these rodlike entities in crystals **1** (E- and N-forms) and **4** are virtually parallel to each other; the distance between the long-axial of the closest neighboring molecules is ca. 5.4, 5.2, and 4.9 Å for **1** (E-form), **1** (N-form) and **4**, respectively. Assuming that the nearest interacting lumophore acts as an energy trap for the molecular crystal upon UV excitation, the geometry of adjacent lumophores in the crystal lattice deserve close scrutiny. A correlation between the solid-state emission properties and crystal packing is tentatively proposed below.

The molecular dipoles of the closest neighboring lumophores are arranged in a head-to-tail fashion in **1** (E-form) but in a slipped manner in **1** (N-form) and **4**. On the other hand, the molecular planes of the two lumophores are coplanar in **1** (E-form) and nearly parallel in **4**, but almost perpendicularly tilted (end-on) in **1** (N-form). In view of the fact that **1** (E-form) and **4** are highly emissive, whereas **1** (N-form) is virtually non-emissive at 298 K, we infer that the angle between the two molecular planes of the interacting lumophores (θ in Figure 9) is linked to the emissive properties of these solids; i.e., when θ deviates significantly from 0 or 180°, the emission becomes diminished.

Interestingly, the above-mentioned angle θ in these crystals is related to the C−H···π(C≡C) contacts between neighboring molecules. As originally reported by Mingo and co-workers,[8a] this type of weak interaction is ubiquitous in gold(I) acetylide complexes and is constructed from an acidic proton and the electron-rich Au−C≡C moiety. There are two identical C−H···π(C≡C) contacts between adjacent lumophores in **1** (E-form), whereas only one such interaction is observed in **1** (N-form). When the substituents of the phosphine ligand is changed from Cy_3P to Ph_3P, or the arylacetylide from 4-nitro- to pentafluorophenylacetylide, such C−H···π(C≡C) contacts are absent. Thus, the crystal packing arrangements derived from these weak C−H···π(C≡C) contacts are crucial for the different emission properties of the two polymorphs of **1**.

Exciton-Coupling Interactions? In the crystal lattice of **1**, the arylacetylide lumophores are packed into dimers or infinite chains through weak C−H···π(C≡C) contacts, hence excitonic interactions become possible. It is apparent that both electronic

(19) Thalladi, V. R.; Weiss, H. C.; Bläser, D.; Boese, R.; Nangia, A.; Desiraju, G. R. *J. Am. Chem. Soc.* **1998**, *120*, 8702−8710.

and crystal packing factors cooperatively affect the excitonic interactions of arylacetylide units in the solid state. Because the triplet emissive excited state of **1** is intraligand charge-transfer in nature, we can assume that the polarization of the singlet transition dipole moment occurs in the molecular plane while the polarization of the triplet one is perpendicular to the molecular plane.[14a] Thus, the dihedral angle between the triplet transition dipole moment vectors of the two 4-nitrophenylacetylide moieties correlates to the angle θ in Figure 9. As described in previous studies on excitonic coupling-induced split-type Cotton effects in circular dichroic spectra,[20] the amplitude of excitonic coupling between two neighboring chromophores is dependent on the dihedral angle between the electronic transition dipole moment vectors of the two chromophores; if the angle between the two coupled transition dipoles is approximately 70°, exciton splitting is maximized; on the other hand, if the two transition dipoles are parallel ($\theta = 0$ or 180°), no exciton splitting is observed. Bearing this in mind, it is notable that there could be significant excitonic interaction(s) between neighboring 4-nitrophenylacetylide moieties in the N-form of **1** ($\theta = 79°$) but negligible excitonic coupling in the E-form of **1** ($\theta \approx 180°$) and in **4** ($\theta \approx 0°$). We suggest that the excitonic coupling in the N-form of **1** results in the transfer of excitation energy to nonradiative energy traps that are presumably located at the lattice flaws. These processes are apparently suppressed at low temperatures, as indicated by the substantial enhancement of the emission intensity of **1**(N-form) at 77 K. In view of the efficient spin−orbit coupling conferred by the $[(Cy_3P)Au]^+$ moiety (as evidenced by the ϵ value for the $S_0 \rightarrow T_1$ absorption of **1** in CH_2Cl_2 solution), the triplet excitonic splitting energy for the 0−0 transition in the present study could be substantially larger than that for the anthracene (17 cm^{-1}) and 1,4-dibromonaphthalene (30 cm^{-1}) systems.[21] At this stage, it is nevertheless difficult to assign a tangible meaning to the value of 730 cm^{-1} by which the emission energy of the N-form of **1** is blue-shifted from the E-form at 77 K.

Concluding Remarks

It is apparent that polymorphism can occur in two-coordinate gold(I) complexes supported by phosphine auxiliaries, and aurophilic interactions are not a prerequisite for this phenomenon.[22] In the present study, we have been able to prepare and isolate two distinct polymorphs of the neutral gold(I) 4-nitrophenylacetylide complex with the ancillary Cy_3P ligand, which exhibit highly contrasting phosphorescent characteristics. By comparing the X-ray crystal structures and emission properties of these polymorphic solids and the related complexes **2**−**4**, it is evident that both electronic and crystal packing factors play crucial roles in possible excitonic coupling interactions in this system. These findings not only enrich the diverse luminescent nature of gold(I) complexes, but also provide valuable information for crystal engineering studies of phosphorescent metal-organic compounds.

Experimental Section

General Procedures and Materials. All starting materials were purchased from commercial sources and used as received unless stated otherwise. The solvents used for synthesis were of analytical grade. Details of solvent treatment for photophysical studies have been described earlier.[23] $[(Cy_3P)AuCl]$,[12d] 4-nitrophenylacetylene,[24a] 4-trifluoromethylphenylacetylene,[24a] and pentafluorophenylacetylene[24b] were prepared according to literature methods. ^1H and ^{13}C NMR spectra were recorded on a Bruker Avance 400 or 300 DRX FT-NMR spectrometer (referenced to residual solvent) at 298 K. ^{19}F and ^{31}P NMR spectra were recorded on a Bruker Avance 400 at 298 K. Mass spectra (FAB) were obtained on a Finnigan MAT 95 mass spectrometer. Elemental analyses were performed by Beijing Institute of Chemistry, Chinese Academy of Sciences. UV−vis spectra were recorded on a Perkin-Elmer Lambda 19 UV/vis spectrophotometer. Emission spectra were obtained on a SPEX Fluorolog-2 Model F11 fluorescence spectrophotometer. Emission lifetime measurements were performed with a Quanta Ray DCR-3 pulsed Nd:YAG laser system (pulse output 355 nm, 8 ns).

Synthesis. Complexes **1**−**4** were prepared by reacting $[(Cy_3P)AuCl]$ or $[(Ph_3P)AuCl]$ with 4-R−$C_6H_4C{\equiv}CH$ (R = NO_2, CF_3) or $C_6F_5C{\equiv}CH$ in the presence of NaOMe in CH_2Cl_2/MeOH (1/1, v/v) and purified with flash chromatography (neutral alumina, CH_2Cl_2 as eluent).

$[(Cy_3P)AuC{\equiv}CC_6H_4$-4-$NO_2]$ (1): Anal. Calcd. for $C_{26}H_{37}NO_2PAu$: C, 50.16; H, 5.83; Found: C, 50.11; H, 6.10%. FAB MS: *m*/*z* 624 [M^+]. ^1H NMR ($CDCl_3$): $\delta = 8.10$ (d, 2H, $^3J = 8.7$ Hz), 7.58 (d, 2H, $^3J = 8.7$ Hz), 2.10−1.18 (m, 33H, Cy). $^{31}P\{^1H\}$ NMR ($CDCl_3$): $\delta = 56.4$.

$[(Cy_3P)AuC{\equiv}CC_6H_4$-4-$CF_3]$ (2): Anal. Calcd. for $C_{27}H_{37}F_3PAu$: C, 50.16; H, 5.77; Found: C, 50.07; H, 6.09%. FAB MS: *m*/*z* 647 [M^+]. ^1H NMR ($CDCl_3$): $\delta = 7.58$ (d, 2H, $^3J = 8.1$ Hz), 7.48 (d, 2H, $^3J = 8.3$ Hz), 2.08−1.24 (m, 33H, Cy). $^{19}F\{^1H\}$ NMR ($CDCl_3$): $\delta = -62.5$. $^{31}P\{^1H\}$ NMR ($CDCl_3$): $\delta = 56.4$.

$[(Cy_3P)AuC{\equiv}CC_6F_5]$ (3): Anal. Calcd. for $C_{26}H_{33}F_5PAu$: C, 46.72; H, 4.98; Found: C, 47.01; H, 4.75%. FAB MS: *m*/*z* 669 [M^+]. ^1H NMR ($CDCl_3$): $\delta = 2.05-1.25$ (m, 33H, Cy). $^{19}F\{^1H\}$ NMR ($CDCl_3$): $\delta = -141.7$ (d, 2F, $J = 22.4$ Hz), −162.1 (t, 1F, $J = 22.4$ Hz), −166.3 (t, 2F, $J = 22.4$ Hz). $^{31}P\{^1H\}$ NMR ($CDCl_3$): $\delta = 56.5$.

$[(Ph_3P)AuC{\equiv}CC_6H_4$-4-$NO_2]$ (4): Anal. Calcd. for $C_{26}H_{19}NO_2PAu$: C, 51.58; H, 3.16; Found: C, 51.75; H, 3.49%. FAB MS: *m*/*z* 606 [M^+]. ^1H NMR ($CDCl_3$): $\delta = 8.13$ (d, 2H, $^3J = 8.4$ Hz), 7.60−7.49 (m, 17H). $^{31}P\{^1H\}$ NMR ($CDCl_3$): $\delta = 56.4$.

X-ray Crystallography. All single crystals were obtained by slow diffusion of Et_2O vapor into a CH_2Cl_2 solution. Data were collected on a MAR diffractometer with a 300 mm image plate detector using monochromatized Mo Kα radiation ($\lambda = 0.71071$ Å). Data collection was made with 3° oscillation step of φ, 300 s exposure time and scanner distance at 120 mm. The images were interpreted and intensities

(20) Harada, N.; Nakanishi, K. *Circular Dichroic Spectroscopy: Exciton Coupling in Organic Stereochemistry*; University Science Books: Mill Valley and Oxford University Press: Oxford, 1983.
(21) (a) Avakian, P.; Ern, V.; Merrifield, R. E.; Suna, A. *Phys. Rev.* **1968**, *165*, 974−980. (b) Hochstrasser, R. M.; Whiteman, J. D. *J. Chem. Phys.* **1972**, *56*, 5945−5958. (c) Pope, M.; Swenberg, C. E. *Electronic Processes in Organic Crystals and Polymers*; Oxford University Press: New York, 1999.
(22) (a) Lock, C. J. L.; Turner, M. A. *Acta Crystallogr.* **1987**, *C43*, 2096−2099. (b) Houlton, A.; Mingos, D. M. P.; Murphy, D. M.; Williams, D. J.; Phang, L. T.; Hor, T. S. A. *J. Chem. Soc., Dalton Trans.* **1993**, 3629−3630. (c) Fackler, J. P., Jr.; Staples, R. J.; Khan, M. N. I.; Winpenny, R. E. P. *Acta Crystallogr.* **1994**, *C50*, 1020−1023. (d) Bowmaker, G. A.; Brown, C. L.; Hart, R. D.; Healy, P. C.; Rickard, C. E. F.; White, A. H. *J. Chem. Soc., Dalton Trans.* **1999**, 881−889. (e) Leznoff, D. B.; Rancurel, C.; Sutter, J.-P.; Rettig, S. J.; Pink, M.; Paulsen, C.; Kahn, O. *J. Chem. Soc., Dalton Trans.* **1999**, 3593−3599. (f) Smyth, D. R.; Vincent, B. R.; Tiekink, E. R. T. *Crystal Growth & Design* **2001**, *1*, 113−117.
(23) Chan, S. C.; Chan, M. C. W.; Che, C. M.; Wang, Y.; Cheung, K. K.; Zhu, N. *Chem. Eur. J.* **2001**, *7*, 4180−4190.
(24) (a) Takahashi, S.; Kuroyama, Y.; Sonogashira, K.; Hagihara N. *Synthesis* **1980**, 627−630. (b) Zhang, Y. D.; Wen, J. X. *Synthesis* **1990**, 727−728.
(25) *DENZO*. In *The HKL Manual−A Description of Programs DENZO, XDISPLAYF and SCALEPACK*, written by Gewirth, D. with the cooperation of the program authors Otwinowski, Z. and Minor, W. Yale University: New Haven, USA, 1995.
(26) *SIR-97*: Altomare, A.; Burla, M. C.; Camalli, M.; Cascarano, G.; Giacovazzo, C.; Guagliardi, A.; Moliterni, A. G. G.; Polidori, G.; Spagna, R. A new tool for crystal structure determination and refinement. *J. Appl. Crystallogr.* **1998**, *32*, 115.
(27) *SHELXL-97*: Sheldrick, G. M. SHELX97, Programs for Crystal Structure Analysis (Release 97−2), University of Goetingen, Germany, 1997.
(28) *SHELXS-97*: Sheldrick, G. M. SHELX97, Programs for Crystal Structure Analysis (Release 97−2), University of Goetingen, Germany, 1997.

integrated using program *DENZO*.[25] The structure was solved by direct methods employing *SIR-97*[26] except for 4 (*SHELXS-97*[27]). The Au, P and many non-H atoms were located according to direct methods and successive least-squares Fourier cycles. Positions of other non-H atoms were found after successful refinement by full-matrix least-squares using *SHELXL-97*[28] program. In the final stage of least-squares refinement, all non-H atoms were refined anisotropically. The positions of H atoms were calculated based on riding mode with thermal parameters equal to 1.2 times that of the associated C atoms and participated in the calculation of final R-indices. One crystallographic asymmetric unit consists of one formula unit for all crystal structures in the present study.

Acknowledgment. We are grateful for financial support from The University of Hong Kong and the Research Grants Council of Hong Kong SAR, China [HKU 7039/03P]. W.L. acknowledges the receipt of studentship from The University of Hong Kong.

Supporting Information Available: Additional crystallographic plots and CIFs; supplementary absorption and emission spectra. This material is available free of charge via the Internet at http://pubs.acs.org.

JA0382415